

Copyright © 1993, by the author(s).  
All rights reserved.

Permission to make digital or hard copies of all or part of this work for personal or classroom use is granted without fee provided that copies are not made or distributed for profit or commercial advantage and that copies bear this notice and the full citation on the first page. To copy otherwise, to republish, to post on servers or to redistribute to lists, requires prior specific permission.

**EXPERIMENTAL ANALYSIS OF 1-D  
MAPS FROM CHUA'S CIRCUIT**

by

N. F. Rul'kov and A. R. Volkovskii

Memorandum No. UCB/ERL M93/29

1 March 1993

**EXPERIMENTAL ANALYSIS OF 1-D  
MAPS FROM CHUA'S CIRCUIT**

by

N. F. Rul'kov and A. R. Volkovskii

Memorandum No. UCB/ERL M93/29

1 March 1993

**ELECTRONICS RESEARCH LABORATORY**

College of Engineering  
University of California, Berkeley  
94720

TITLE PAGE 3

---

This work is supported in part by the Office of Naval Research under grant N00014-89-J-1402 and the National Science Foundation under grant MIP-9001336.

**EXPERIMENTAL ANALYSIS OF 1-D  
MAPS FROM CHUA'S CIRCUIT**

by

N. F. Rul'kov and A. R. Volkovskii

Memorandum No. UCB/ERL M93/29

1 March 1993

**ELECTRONICS RESEARCH LABORATORY**

College of Engineering  
University of California, Berkeley  
94720

---

This work is supported in part by the Office of Naval Research under grant N00014-89-J-1402 and the National Science Foundation under grant MIP-9001336.

# Experimental analysis of 1-D maps from Chua's circuit

N.F.Rul'kov and A.R.Volkovskii

*Radio physical Dpt., Nizhni Novgorod University,  
23,Gagarin Av.,603600 Nizhni Novgorod,RUSSIA.*

## Abstract

Bifurcation analysis by means of a 1-D return map obtained experimentally from Chua's circuit is presented. It is experimentally demonstrated that a *homoclinic bifurcation* associated with the stationary point at the origin of the phase space precedes the birth of the double-scroll Chua's attractor.

## 1. Introduction

Chua's circuit is known as the simplest and deeply studied nonlinear electronic system with chaotic dynamics (see the extensive Bibliography in reference 1). The robustness, simplicity and low cost features of Chua's circuit make it extremely useful for the development and testing of experimental methods for investigating nonlinear systems with chaotic dynamics. The main goal in such studies is the determination of the main bifurcation mechanisms which are responsible for the transition from regular dynamics to chaotic behavior and its subsequent evolutions.

It has been shown in a number of numerical simulations <sup>2,3</sup> that due to the strong dissipative compression of the phase volume the behavior of the trajectories of some attractors in Chua's circuit can be

modeled by means of a *one-dimensional (1-D) return map*. The analysis of return maps can be made much more efficient in the experimental investigation of bifurcation scenarios and chaos in electronic circuits if the curve generated by the return map is automatically plotted by an experimental set up <sup>4</sup>.

In this paper we present some results on the application of 1-D return maps for demonstrating experimentally some basic nonlinear dynamics of Chua's circuit. In our experiments we use the Chua's circuit described in reference 5 with the following parameter values for the linear elements:  $L=84mH$  ,  $C_1=56nF$  and  $C_2=656nF$ ; precision 5%. The parameter values for Chua's diode were chosen to be the same as in reference 5. The value of the variable resistance  $R$  was used as a control parameter. The experimental setup for visualizing the Poincare cross section of attractors, and for plotting the 1-D map was discussed in reference 4.

By tuning the variable resistance  $R$  from  $2000\Omega$  continuously towards zero, Chua's circuit exhibits experimentally a sequence of bifurcations from a stable stationary state to an Andronov-Hopf bifurcation, to a period-doubling cascade, and finally to a chaotic attractor.

## 2. Contraction of the 1-D Return Map

Immediately before the first period-doubling bifurcation, the projection of the stable limit cycle (from the Andronov-Hopf bifurcation) onto the  $(V_{C_1}, V_{C_2})$ -plane is shown in Fig.1. The solid black dot on the trajectory marks the point where the trajectory intersects the chosen Poincaré section  $\Sigma$  defined as a plane located in the phase space and *transversal* to the trajectories of attractors being observed<sup>4</sup>.



Let  $t_n$ ,  $n=1,2,\dots$  denote the consecutive times whenever a trajectory returns and passes through the Poincaré plane  $\Sigma$ . Each such intersection  $(V_{C1}(t_n), V_{C2}(t_n))$  is called a *return point* and is identified by a black dot on the trajectory as shown in Fig.2,3. From the coordinates of two consecutive return points at  $t=t_n$  and  $t=t_{n+1}$ , we plot the 1-D map  $(V_{C1}(t_n), V_{C1}(t_{n+1}))$  as presented also in Fig.2,3. In order to simplify our description of the attractor bifurcations let us define  $X_n=V_{C1}(t_n)$  so that the 1-D map obtained in our experiments can be written simply as  $X_{n+1}=F(X_n, R)$ . While the 1-D map  $F(., R)$  is a piecewise-continuous curve, our present experimental set up can obtain only a subset of points lying on the curve.

#### A. Period Doubling

As we decrease the resistance  $R$ , the evolution of the various attractors represented by their projections onto the  $(V_{C1}, V_{C2})$ -plane, and by the Poincaré cross sections are shown in Figs.2 and 3. In each case, the points where the attractor intersect the Poincaré section are automatically displayed as a subset of the associated 1-D map. This subset will consist of  $m$  points for a periodic orbit having  $m$  intersections, called a period- $m$  orbit, or an infinite number of intersections (where its limit set has a fractal dimension between 1 and 2) for a chaotic attractor. Due to the influence of physical and measurement *noise* only a limited number of period-doubling bifurcations can be observed in experiments before chaos emerges. However, the shape of the experimentally plotted subset of points on the 1-D map of the attractors (see Fig.2c,d) will enable us to conclude that this particular transition to chaos and the topological properties of the attractors are in accordance with the Feigenbaum scenario.

## B. Intermittency and Periodic Windows

The existence of a minimum point on the return function  $F(.)$  ( $F'(X_{min})=0$ ,  $F''(X_{min})\neq 0$ ) is responsible for the alternate appearance of chaotic and stable periodic regimes (called periodic windows) as we tune the parameter  $R$ . As an example a stable limit cycle  $3T_+$  corresponding to a period-3 window is shown in Fig.2f. An *intermittent phenomenon*, which is a form of *chaos*, is observed *before* the appearance of this period-3 limit cycle as  $R$  decreases, as shown in Fig.2e. This form of chaos is called an *intermittency* because except for the *random* appearance of *brief* intervals of spurious bursts, the time waveforms are virtually periodic. In the cross section of Fig.2e, the bursts corresponds to the short "arc" crossing the fuzzy period-3 orbit. The period-3 window is followed by a period-doubling bifurcation sequence of this period-3 cycle which leads to the appearance of the chaotic attractors shown in Fig.2g,h. In view of the odd symmetry of the vector-field in the phase space of Chua's circuit<sup>2</sup>, for every attractor presented above we can observe a coexisting "twin" attractor, often just by switching the circuit on and off.

## C. Crisis and homoclinicity

When the parameter  $R$  crosses some critical value  $R_{cr}$  (in our experiments  $R_{cr}\cong 1640\Omega$ ) the twin chaotic attractors  $CA_+$  and  $CA_-$  collided with each other, thereby giving rise to a *crisis phenomenon*<sup>6</sup> which gave birth to the odd symmetric chaotic attractor  $CA$  (called double-scroll Chua's attractor) shown in Fig.3a. Observe that the 1-D map of  $CA$  (obtained from the cross section shown in this figure) has a discontinuity at  $X_n=a$ . This results from the nature of the trajectory motions in the vicinity of the saddle-focus  $O_0$  which is located at the

origin of the phase space.

The trajectories originating from a Poincare section of the attractor are separated by the two-dimensional stable manifold of the saddle-focus  $O_0$  into two parts; namely,  $A\{X \geq a\}$  and  $B\{X < a\}$ . Until their next intersections with the Poincare plane the behavior of the trajectories from part  $A$  before and after the crisis are similar. As a result the part of the 1-D map  $F(X,R)$  with  $X > a$  undergoes only a small variation. However, before the trajectories from part  $B$  return to the Poincare section, they can have rather complicated behaviors in the left part of the phase space. This behavior gives rise to the complicated oscillatory structure of  $F(X,R)$  in the domain  $X < a$ , as shown in Fig3.

The crisis bifurcation of the twin spiral Chua's attractors  $CA_+$  and  $CA_-$  takes place at some bifurcation parameter  $R_{cr}$  when a trajectory belonging to the attractor  $CA_+$  and originating from the minimum point on the 1-D map is mapped into the point  $a$ , i.e.,  $a = F(X_m, R_{cr})$ , where  $X_m = \min\{F(X, R_{cr}) \mid X \in CA_+\}$ . For  $R < R_{cr}$ , all trajectories originating from the interval  $[X_m, a]$  belong to part  $B$ .

A detailed analysis of the 1-D map and the topological properties of the trajectories in the phase space enable one to make the following conclusions: Before the crisis, when  $a < X_{min} = \min\{F(X, R) \mid X > a\}$ , the two-dimensional stable manifold of  $O_0$  ( i.e.  $W_2^s$ ) separates the basins of the two spiral Chua's attractors  $CA_+$  and  $CA_-$ . In this case any trajectory from one side of the manifold can never go to the other side. Observe that in the 1-D map model the entire stable manifold  $W_2^s$  is mapped into the point  $a$ , see reference 2 . After the crisis, the trajectories of the symmetric double-scroll Chua's attractor  $CA$  can go from one side of  $W_2^s$  to the other. This implies that at least one

homoclinic bifurcation associated with the point  $O_0$  must occur before the crisis of  $CA_+$  and  $CA_-$ . In the three-dimensional phase space of Chua's circuit a homoclinic orbit at  $O_0$  is *any* trajectory through  $O_0$  which belongs to both the one-dimensional unstable manifold (which coincides with the unstable eigenvector through  $O_0$  in the middle region) and the two-dimensional stable manifold through the point  $O_0$  simultaneously. From the viewpoint of the 1-D map, a homoclinic orbit at  $O_0$  is *any* trajectory which satisfies the equation  $a=F^{(k)}(a,R_k)$ , where  $k$  is the number of iterations of the function  $F$ , and  $R_k$  is the parameter value of  $R$  corresponding to the occurrence of the homoclinic orbit  $H_k$ .

#### D. Stable periodic orbits and chaotic quasiattractors

Because the return map has many local extremum points (see Fig.3f and 3i), many stable limit cycles can exist in the parameter region corresponding to the spiral Chua's attractor, or to the double-scroll Chua's attractor<sup>7</sup>. Some examples of the periodic orbits having large basins of attraction are shown in Fig.2f and in Fig.3c,d and h.

Stable limit cycles associated with multiple local extrema of 1-D return map can have long periods and extremely complicated yet very narrow basins of attraction. These features made them almost invisible in experiments and in numerical simulations. Despite their local stability any small noise will throw a periodic trajectory out of its basin, and as a result this trajectory will land in a domain of complicated transient motions. In this case the oscillation of the circuit can remain chaotic with the simultaneous co-existence of stable limit cycles in the attractor. This kind of chaotic attractors are called as quasiattractors<sup>8</sup>. The results in Fig.3 can serve as an experimental demonstration of the theory of the spiral-type attractors

which can take place in dynamical systems having a homoclinic orbits from a saddle-focus<sup>9-11</sup>.

Figures 3e,f and g demonstrate some examples of the crises of the chaotic attractors which appeared from the stable periodic orbits shown in Fig.3d and h. These crises can occur from the intersection of the stable and unstable invariant manifolds of odd-symmetric periodic orbits of the saddle type<sup>6</sup>. Our conclusion concerning the existence of saddle periodic orbits comes from the *oscillatory* shape of the return functions, shown in Fig.3f and i.

Finally, we remark that the examples presented above do not exhaust the great varieties of dynamical phenomena which can be observed from a more extensive experimental study of the 1-D map. The results of this on-going research will be reported in a future publication.

The authors would like to thank L.O.Chua for careful reading of the manuscript and a number of useful suggestions.

### References

1. L. O. Chua. "Global unfolding of Chua's circuits", *Memorandum*, Electronics Research Laboratory, University of California, Berkeley, 1992, p.60. See also revised version in *IEEE Transactions on Fundamentals of Electronics, Communications and Computer Science*, Special Issue on Neural Nets, Chaos and Numerics, May 1993.
2. L. O. Chua, M. Komuro and T. Matsumoto, "The double scroll family", *IEEE Transaction on Circuits and Systems* CAS-33 (1986) 1073-1118.
3. M. Genot. "Application of 1-D map from Chua's circuit: A

pictorial guide", *J. of Circuits, Systems and Computers* 3 (1993).

4. A. R. Volkovskii and N. F. Rul'kov. "Use of one-dimensional mappings for an experimental study of the stochastic dynamics of an oscillator", *Sov. Tech. Phys. Lett.* 14 (1988) 656-658.

5. M. P. Kennedy, "Robust OP amp realization of Chua's circuit", *FREQUENZ* 46 (1992) 66-80.

6. V. S. Afraimovich, "Internal bifurcations and crises of attractors", *Nonlinear Waves: Structures and Bifurcations* [in Russian] Nauka, Moscow, 1987, p.189-213.

7. P. Glendinning and C. Sparrow, "Local and global behavior near homoclinic orbits", *Journal of Statistical Physics* 35 (1984) 645-695.

8. V. S. Afraimovich and L. P. Shil'nikov, "Strange attractors and quasi-attractors", *Dynamics and Turbulence* Pitman, New York, 1983, p 1-34.

9. L. P. Shil'nikov, "A contribution to the problem of the structure of an extended neighborhood of a rough equilibrium state of saddle-focus type", *Math. USSR Sbornik* 10 (1970) 91-102.

10. I. M. Ovsyannikov and L. P. Shil'nikov, "On systems with a homoclinic curve of the saddle-focus", *Matem. Sbornik* ,130 (1986) p.552-570. English transl. in *Math. USSR Sbornik* 58 (1987) p.557-574.

11. I. M. Ovsyannikov and L. P. Shil'nikov, "Systems with homoclinic curve of the multi-dimensional saddle-focus and spiral chaos", *Matem. Sbornik*, 182 (1991) p.1043-1073. English transl.in *Math.USSR Sbornik* 73 (1991) p.415-443.

### Figure captions

Fig.1 Projection of one of the two asymmetric periodic orbits onto the  $(V_{C1}, V_{C2})$ -plane, with  $R=1689\Omega$ . The location of the Poincaré section plane  $\Sigma$  in the phase space is shown schematically by a small rectangle. Since this orbit intersects the Poincaré section at only one point (black dot), we call this limit cycle a *period-one orbit*.

Fig.2 Projections of various attractors onto the  $(V_{C1}, V_{C2})$ -plane where the black dots and lines on the left are the intersections with the Poincaré section. The corresponding points and lines are replotted in the right by electronic circuitry such that each pair of successive intersection points  $(X_n, X_{n+1})$  becomes the coordinates of a point on the 1-D return map associated with the chosen Poincaré section. (a)  $R=1679\Omega$ ,  $2T_+$ ; (b)  $R=1675\Omega$ ,  $4T_+$ ; (c)  $R=1672\Omega$ , two-band  $CA_+$ ; (d)  $R=1668\Omega$ , one-band  $CA_+$ ; (e)  $R=1660\Omega$ , intermittency; (f)  $R=1658\Omega$ ,  $3T_+$ ; (g)  $R=1647\Omega$ ,  $CA_+$ ; (h)  $R=1645\Omega$ ,  $CA_+$ . The code  $nT_+$  denotes a *period-n orbit* located in the right hand side of the origin. The code  $CA_+$  denotes a chaotic attractor located in the right hand side of the origin.

Fig.3 Projections of various symmetric attractors onto the  $(V_{C1}, V_{C2})$ -plane (left) and their corresponding 1-D maps (right). (a)  $R=1636\Omega$ , double scroll; (b)  $R=1595\Omega$ , double scroll; (c)  $R=1529\Omega$ ,  $6T_S$ ; (d)  $R=1419\Omega$ ,  $2T_S$ ; (e)  $R=1417\Omega$ ,  $CA$ ; (f)  $R=1416\Omega$ ,  $CA$ ; (g)  $R=1415\Omega$ ,  $CA$ ; (h)  $R=1414\Omega$ ,  $2T_S$ ; (i)  $R=1409\Omega$ ,  $CA$ . The code  $nT_S$  denotes a symmetric period- $n$  orbit.

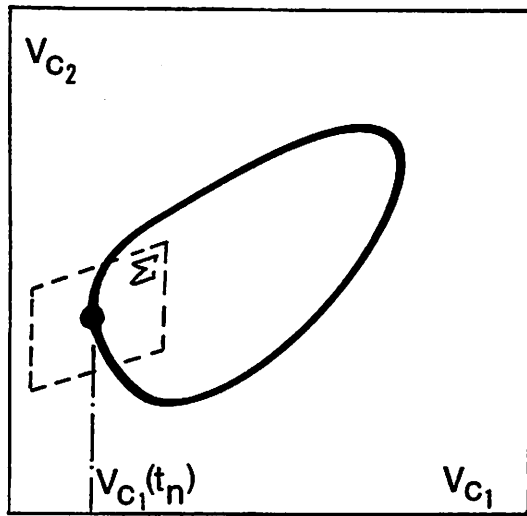
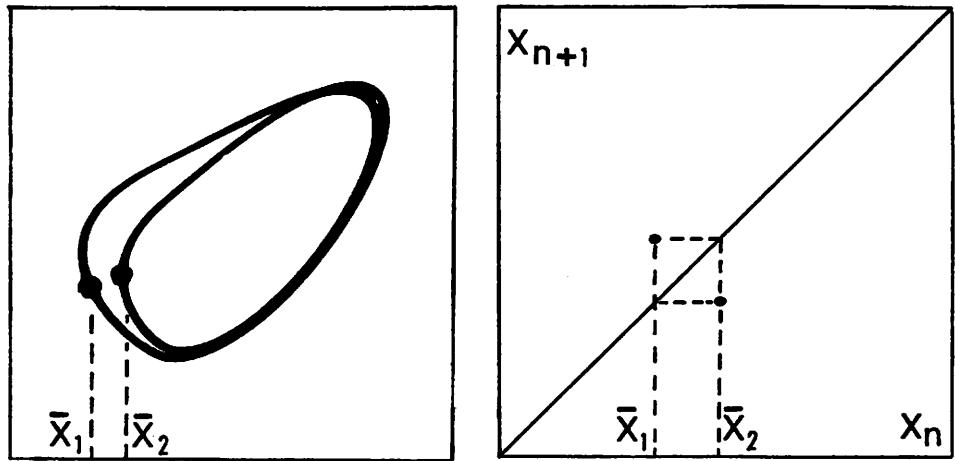
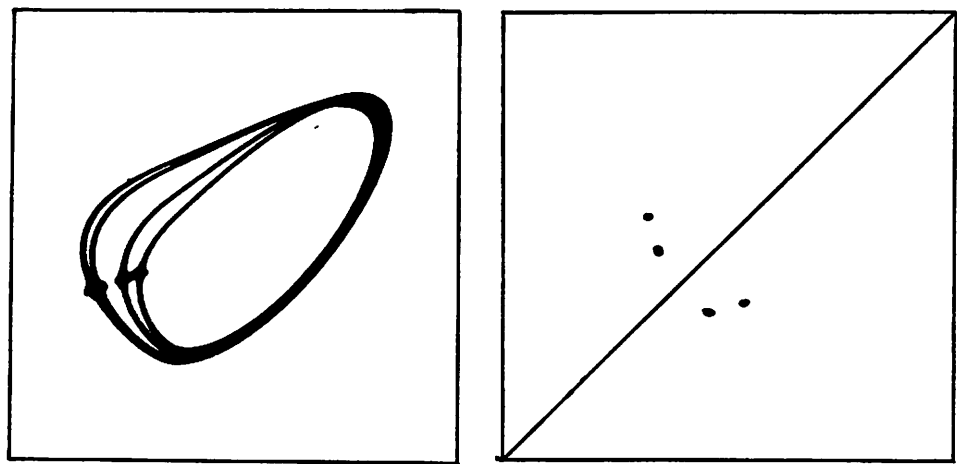


Fig.1





a



b

Fig. 2

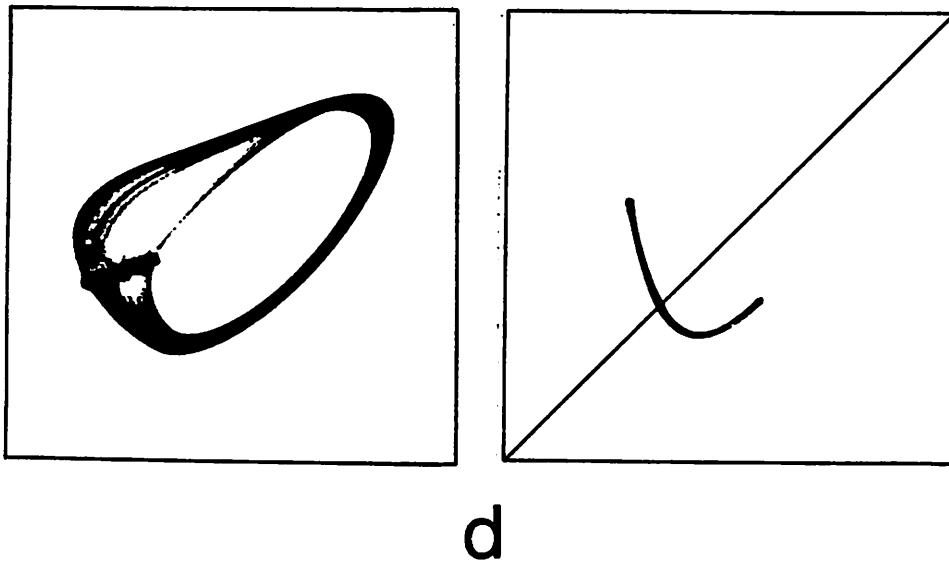
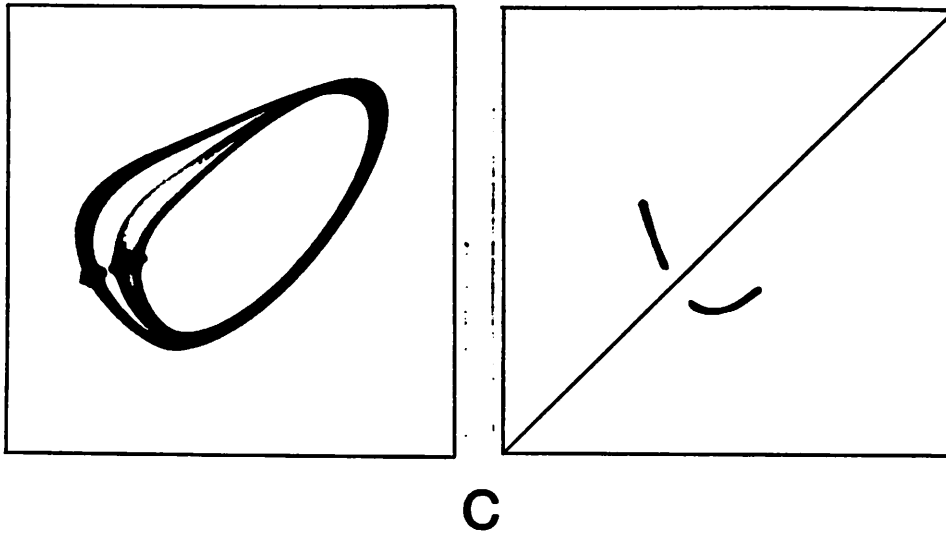
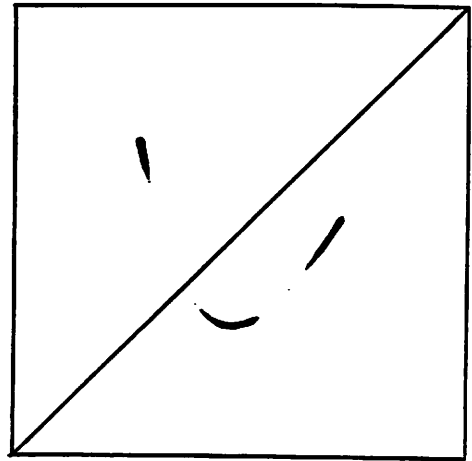
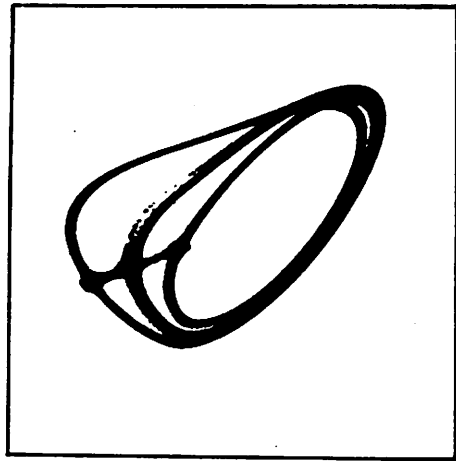
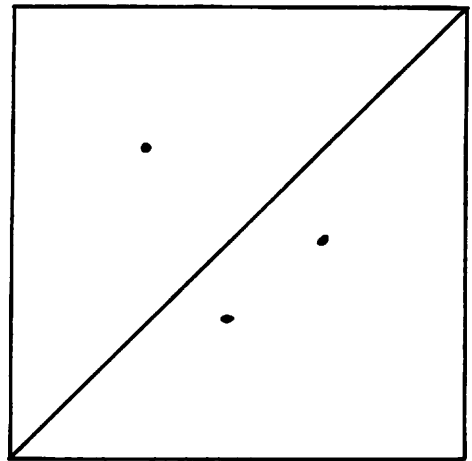
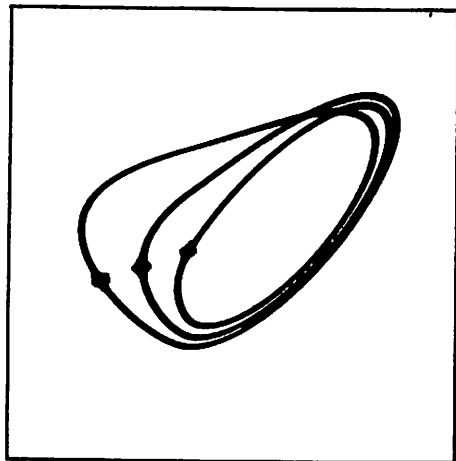


Fig. 2

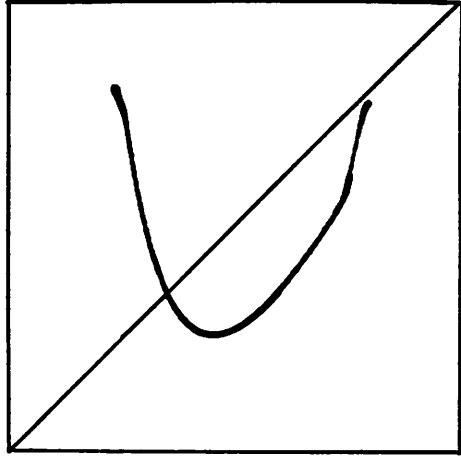
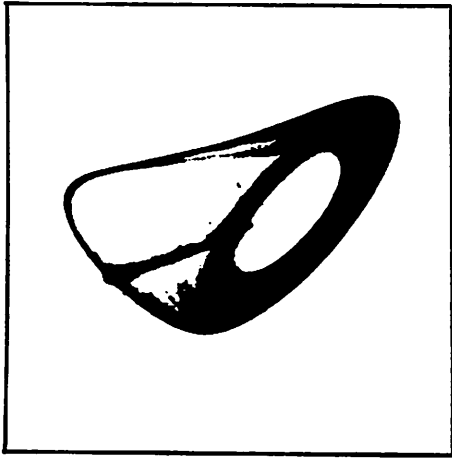


e

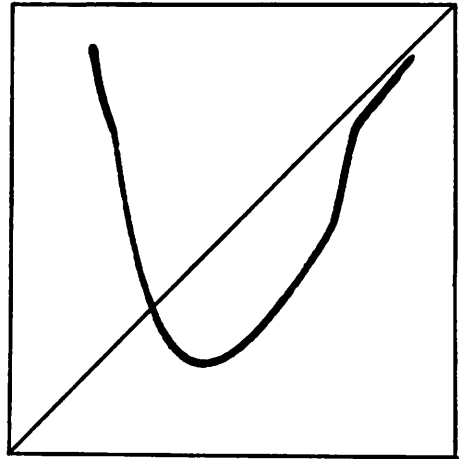
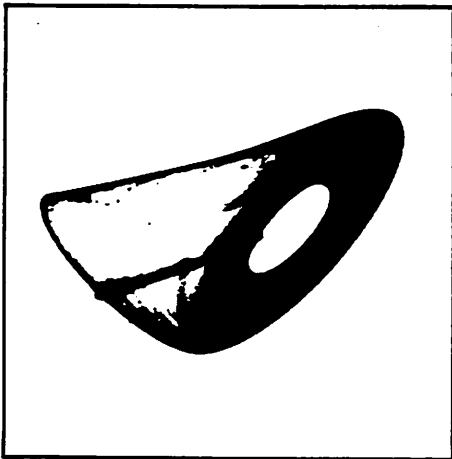


f

Fig. 2

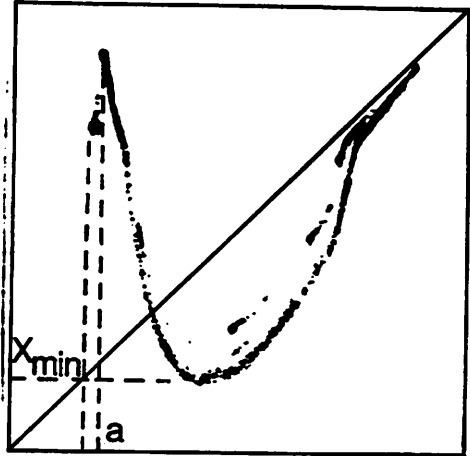
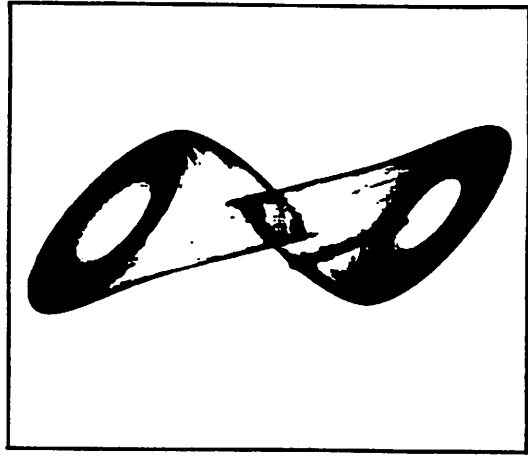


g

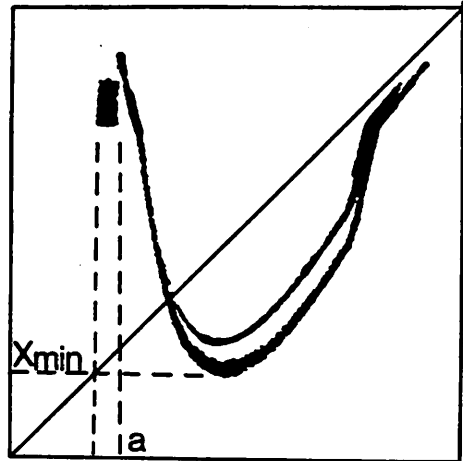
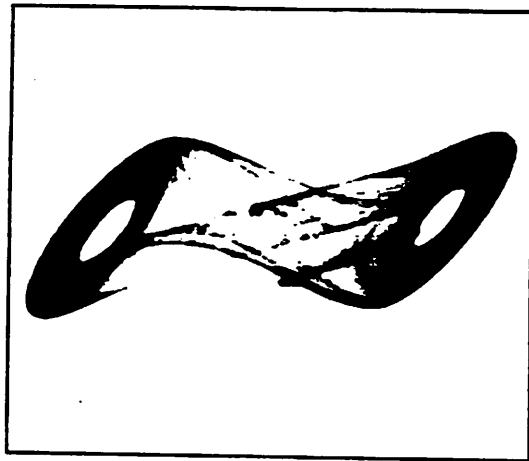


h

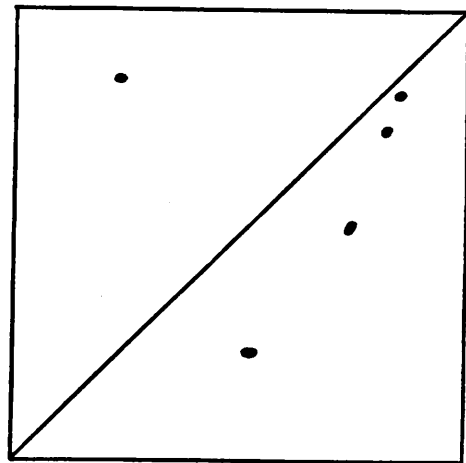
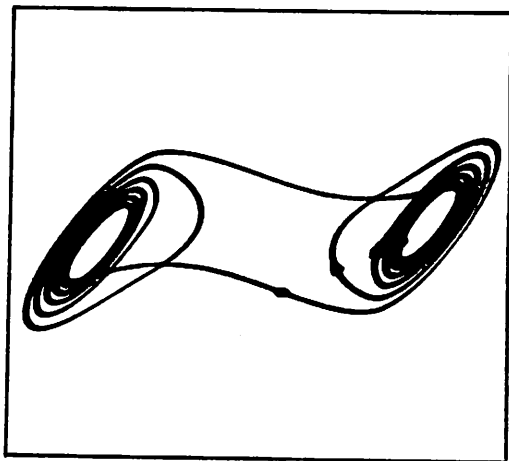
Fig. 2



a

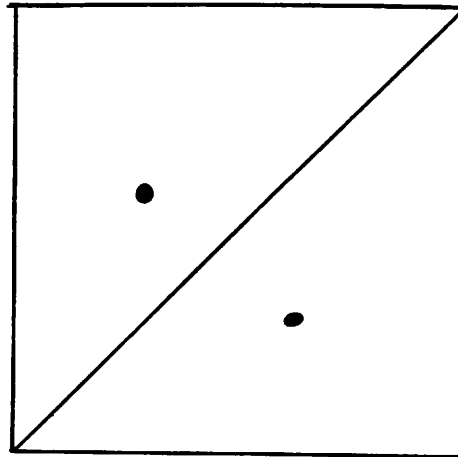
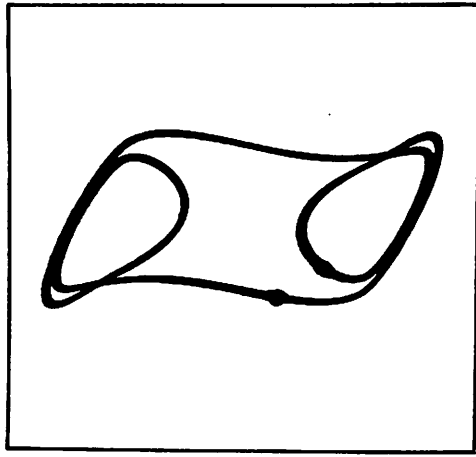


b

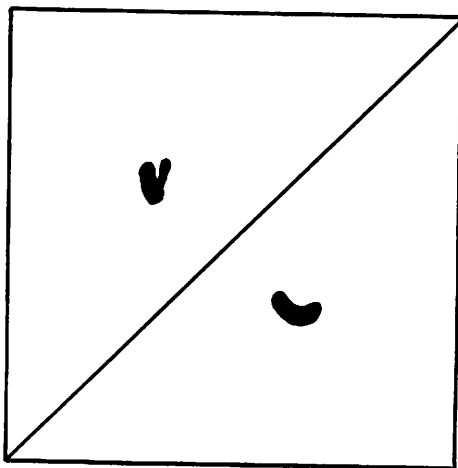
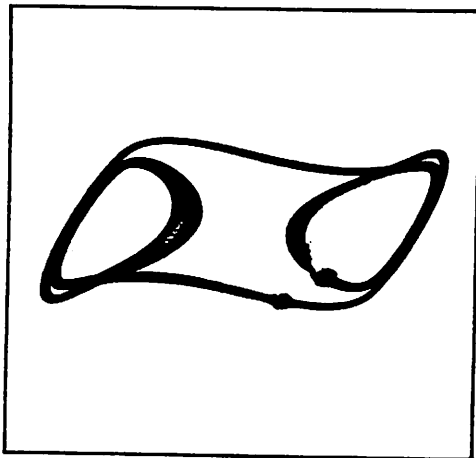


c

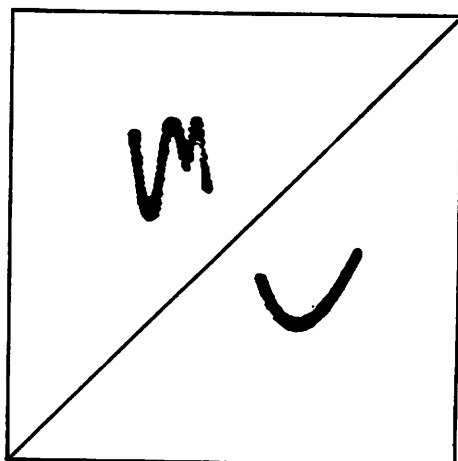
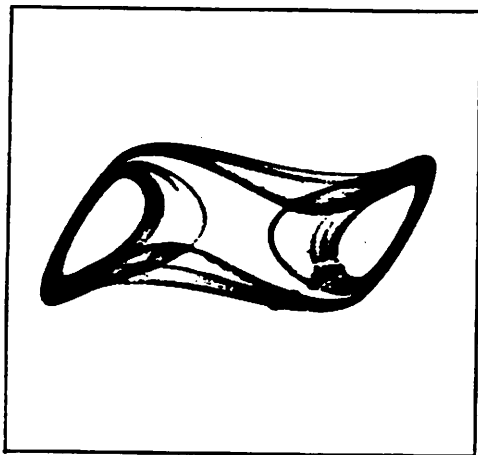
Fig. 3



d

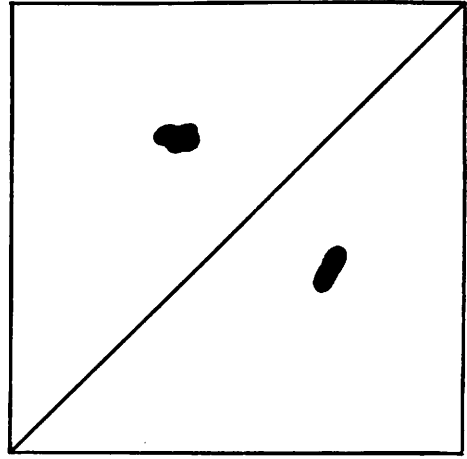
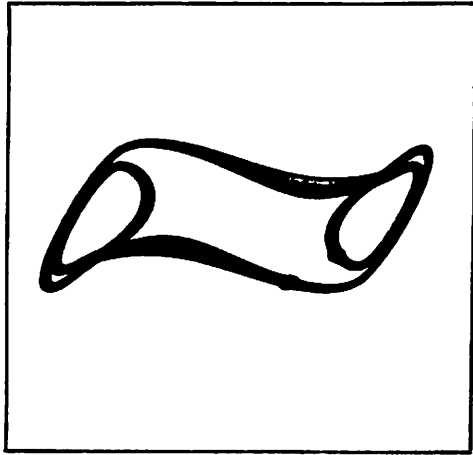


e

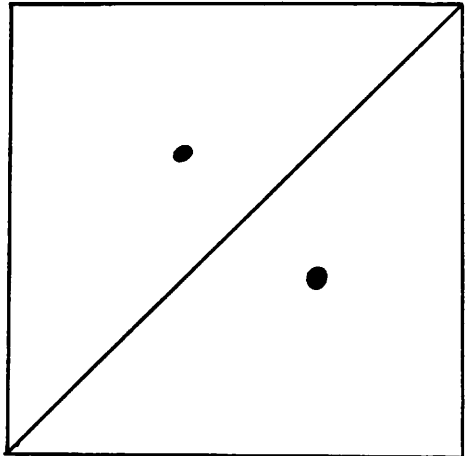
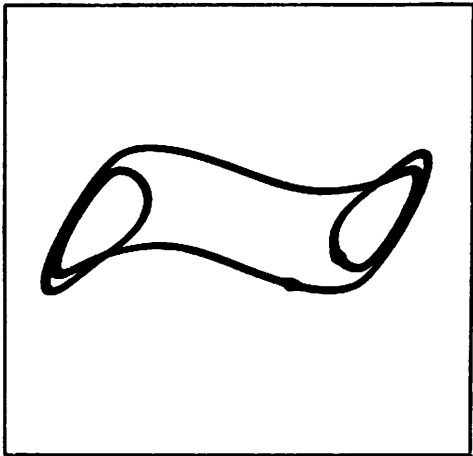


f

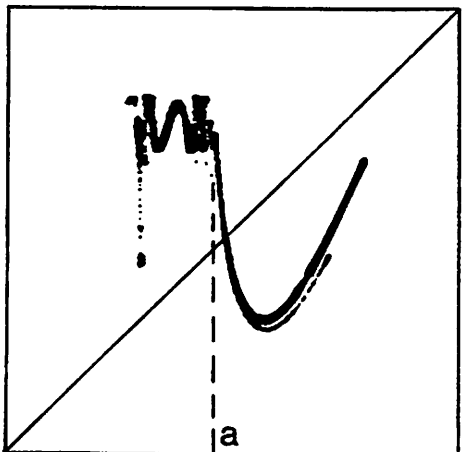
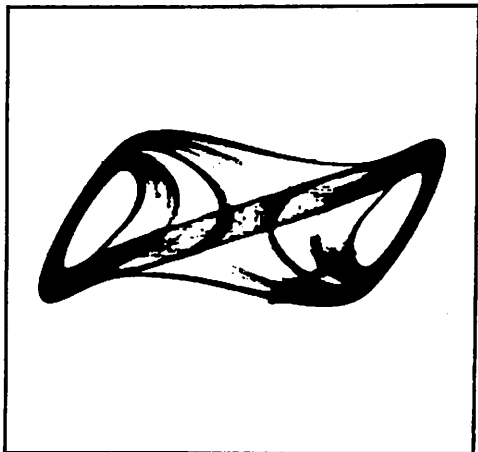
Fig. 3



g



h



i

Fig. 3